SF2A 2016
L. Cambrésy, M. Deleuil, E. Pécontal, C. Reylé, J. Richard, L. Tresse and I. Vauglin (eds)

STELLAR FEEDBACK DURING THE REIONIZATION WITH EMMA

N. Deparis[1], D. Aubert[1] and P. Ocvirk[1]

Abstract. Stellar feedback during the epoch of reionization is a complex problem that is far to be fully understood. The apparition of first stars in the Universe involves highly nonlinear processes that are studied using numerical simulations. We present here a model of star formation, radiation and supernovae feedback, implemented in a new AMR code with fully coupled radiative-hydrodynamic named EMMA. We present a preliminary study concerning the flow of matter and radiation passing through the virial sphere of each halos. We found a class of low-mass halo (less than $10^9 M_\odot$) getting at the same time gas outflow and radiative inflow, suggesting a photo-heating effect.

Keywords: cosmology: dark ages, reionization, first stars - methods: numerical

1 Introduction

Star formation and feedback involve some complex coupling between stars and the intergalactic medium (IGM). By its presence, a star will modify its neighborhood, and then change the state of the medium where futures generation of stars will born. To study this highly nonlinear coupling, we use numerical simulations. Different ways has been explored to implement star formation and feedback (Springel & Hernquist (2003), Stinson et al. (2006), Dubois & Teyssier (2008), Dalla Vecchia & Schaye (2012)). We present one model of star formation, radiative feedback, and supernovae feedback implemented in `EMMA` (Aubert et al. 2015).

During our calibration process, we found that the mass of stellar particle has a drastic effect on how the radiation escapes halos and thus on the reionization history of the simulation. This variation could totally change our interpretation of the simulation, and with the introduction of radiation, we need to take some extra precaution before making conclusions. We also investigate how stellar feedback influences the flow of matter and radiation escaping or falling back around each halo.

2 EMMA

`EMMA` is written with the goal of studying the Epoch of Reionization. A full description of the code is given in Aubert et al. (2015), but we briefly summarize it in this section. It follows the evolution of three distinct physics: dark matter (DM), gas, and light in a fully coupled way.

`EMMA` uses a fully treated tree adaptive mesh refinement (AMR) description. Collisionless dynamics – dark matter and stars – use a particle based representation. A cloud in cell (CIC) projection is used to determined gravitational density field from particles. The Poisson equation is solved using a multigrid relaxation method on the base level, and a Gauss-Seidel relaxation on the sub levels. Hydrodynamics solver is based on a piecewise linear method a la MUSCL-Hancock driven by HLLC Riemann solvers. Finally, the radiation propagation is solved using a moment-based description, with the M1 closure approximation. The chemistry module only computes the cooling and ionization processes of atomic hydrogen in the current version.

[1] Observatoire Astronomique de Strasbourg, CNRS UMR 7550, Universite de Strasbourg, Strasbourg, France

3 Stellar formation and feedback model

The first part of the stellar models is the star formation process, which occurs in three steps. First, we need to define which region are allowed to form stars, then quantify the amount of gas to convert into stars, and do this conversion.

To flag stars forming regions, we use a simple density threshold.

Some authors use much more complex star formation criterion (see eg Kay et al. (2002) for a detailed comparison about star formation criterion). After some tests, we conclude that at the considered scales (our common resolution is around 1kpc), other criteria (like Jeans unstable or convergent flow) do not make a real difference. This behavior is not true anymore for simulations with sub-galactic scale resolution.

We then compute the star formation rate (SFR) of all the flagged region using a simple Schmidt-Kennicutt observational law (Kennicutt 1998) based on the local gas density :

$$\mathrm{SFR} \propto \rho_{gas}^{1.5}. \tag{3.1}$$

We now have the amount of gas to convert into stars. This conversion consists of taking some gas on the grid and convert it into a particle. A newly formed stellar particle can only have a discrete mass depending on a user parameter. For numerical reasons, we use a quantum based description of stellar particles. To go from the continuous process of star formation to a discrete one in the simulation, we draw the number of particles to inject using a Poisson law (Rasera & Teyssier 2006).

Newly born stars will now start their radiative lives. To constrain the type and the amount of radiation stars will emit, we use the Starburst99 model (Leitherer et al. (1999)). It gives us access to the emissivity spectrum of a stellar population of a given initial mass function (IMF). In this study, we use a Top Heavy IMF and a metallicity of Z=0.001.

During our calibration process, we observed a strong dependence of the stellar quantum mass on the reionization history. We observe that injecting one unit of stellar mass if much more efficient – regarding ionization processes – than injecting eight times one eighth of this mass. It seems that the radiation cannot escape from cells containing low mass stars. We made the experiment of executing two runs, one with the recombination processes shut down in cells containing stars, and another one where we let the recombination happen normally. We do this experiment for different stellar masses and observe that for low stellar particle masses ($10^3 \mathrm{M}_\odot$), reionization histories of runs with free recombination processes, are late compared to constrained one. There is no difference for runs with high stellar masses ($7.10^4 \mathrm{M}_\odot$). In this study, we choose to use heavy stellar particles and let the recombination append normally.

After 17Myrs, stars explode in supernovae, injecting $9.7 \cdot 10^{11} \mathrm{J.kg}^{-1}$, and returning 52% of his mass to the IGM. We can either inject the available energy by heating the medium around the explosion or by modifying its velocity. The thermal energy injection is known to be inefficient due to the efficiency of cooling processes. So we developed a kinetic model which inject the energy by the intermediate of ejecta, and by computing the momentum balance in the cell.

4 Halo flow

We develop a tool to analyze what is falling on halos and what is escaping from halos either baryonic matter or radiation. For each halo, we draw a virtual sphere, discretized with Healpix, with a radius corresponding to the associated virial radius and centered on the mass center. The net flow is then compute using :

$$F = \sum_{i=1}^{N} \vec{f_i} \cdot \vec{r_i}, \tag{4.1}$$

with N the number of Healpix point (3072 in this case), $\vec{r_i}$ the radial unit vector at point i and $\vec{f_i}$ the flow of the nearest cell. Normal is oriented outward, so positive values go for outflow and negatives one for inflow. The motion of the center of mass of halos is compensated to reduce environmental effects.

4.1 Hydrodynamical flow

Fig. 1 present results for hydrodynamical flows in a 12 cMpc^3 simulation. This simulation run with a Planck cosmology (Planck Collaboration et al. 2015), and use 256^3 dark matter particles for a mass resolution of

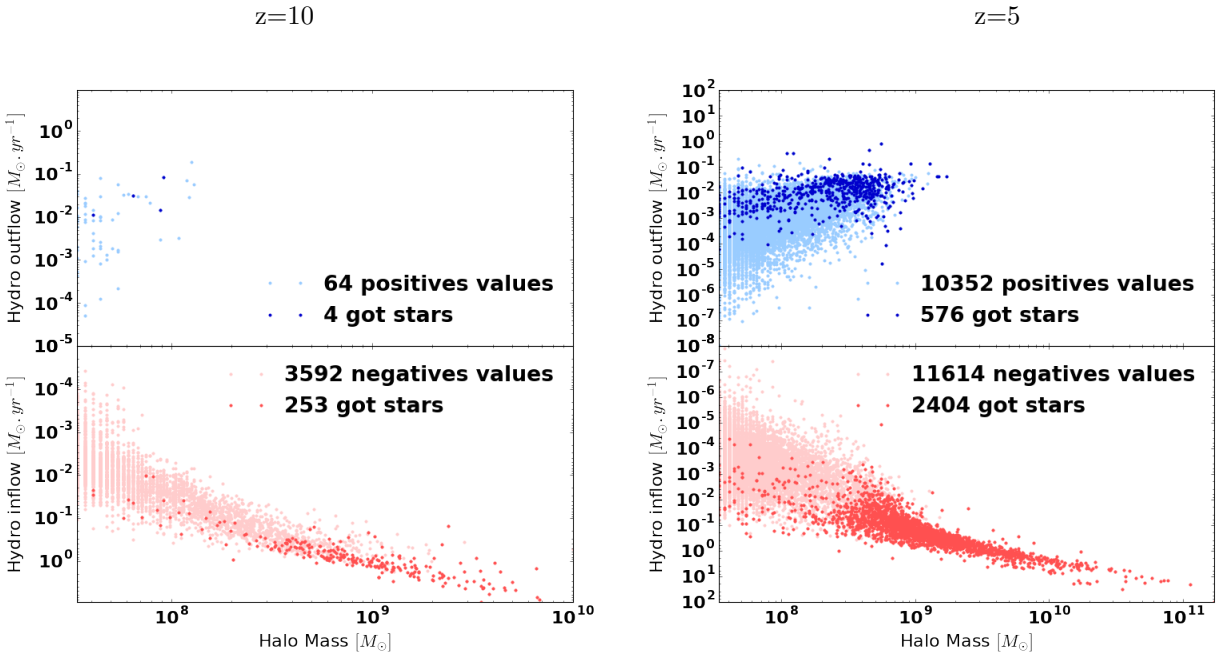

Fig. 1. Hydrodynamical flow of halos at redshift 10 (left) and redshift 5 (right). Positives values are for outflow, dark dots represents halos without stars, light dots represents halos with stars. There is much more low mass halos with gas outflow at z=5 than at z=10. Feedback push the baryon outside of lightest halos, who do not have enough gravitational potential to keep their gas inside their virial radius.

$3.4 \cdot 10^6 M_\odot$. Mesh refinement is allowed until resolution reach 500pc. Stellar quantum mass is set to $7.2 \cdot 10^4 M_\odot$ Results are presented at redshift 10 and 5. We see the apparition of a population of low mass halos that get outflow at z=5. This population is not present at z=10. We see here the baryon escaping from low mass halos that do not have enough gravitational potential to hold their gas, heated by radiation or pushed by supernovae feedback. We made the same run excepting that source does not radiate, and this population was considerably reduced (not shown here). We conclude that this effect is at least partially due to radiative feedback. Moreover, this effect became much stronger after the reionization. So, it suggests an outside-in effect. Galaxies get internal radiative sources, even after the end of the reionization, so if the apparition of this population was due to an inside-out effect, it should be present even before the end of the reionization.

4.2 Radiative flow and escape fraction

The left panel of Fig. 2 present the radiative flow obtain in a 12 $cMpc^3$ - 256^3 simulation at redshift 5. We see a relation between halo masses and outflow quantities: the more the halo is massive, the more it will emit light. Surprisingly, we see a population of halos without stars, with radiative outflow. We are not able to explain it at this time. However, there is a population of halos less massive than $10^{10} M_\odot$ with radiative inflow. The majority (60%) of theses get stars, but still get more radiation from outside sources than from their inner one. Moreover, there is no halos of more than $10^{10} M_\odot$ with net inflow.

Knowing the age of stars belonging to a halo, we can compute the number of photons produced within its virial radius. Right panel of Fig. 2 present the ratio between the number of photons passing through the R200 over the number of photons injected in the halo by stars. To do this computation for each halo, we only get positives value, corresponding to outflow, on its respective Healpix sphere.

We see that the observed escape fraction tends to be low for low mass halos, presents a maximum for halos around $10^{10} M_\odot$, and decrease for heavier halos. The peak value seems to be at the same mass independently of considered redshift. Halos around the peak value, tend to have an escape fraction increasing with time. It may be due to the increasing ionization fraction around halos, letting the radiation escaping.

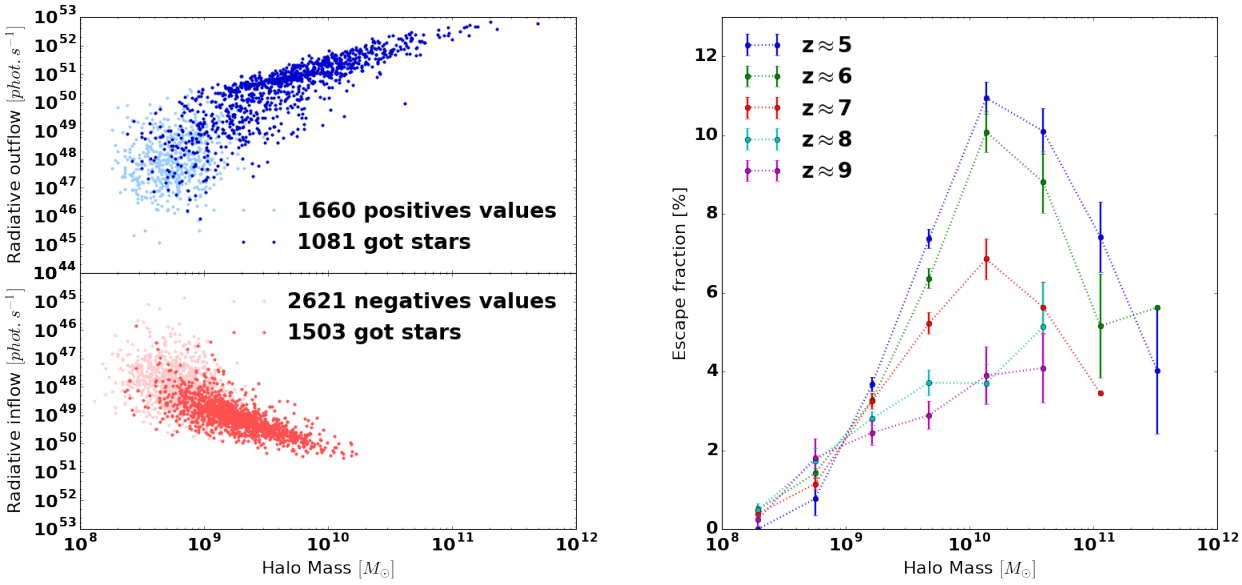

Fig. 2. Radiative flow function of halo mass at redshift 5 (left) and escape fraction function of halo mass function of redshift (right). Dark dots represents halos without stars, light dots represents halos with stars.; We observe a population of low mass halos with radiative inflow and a maximum in the escape fraction for halos around $10^{10}M_{\odot}$.

5 Perspectives

We began to compare halo that get hydrodynamical outflow, and the ones with radiative inflow, to explore the link between theses two populations. The goal is to understand if the photo-heating effect can reduce the SFR in low mass halo by pushing baryons out of their virial radius. This study will also be executed on more resolved boxes to increase the resolution of low mass halos, and on bigger boxes to study the influence of bigger halo.

The momentum based method used for supernovae feedback in this study is revealed to be inefficient to regulate star formation. We are currently working on implementing an other scheme for kinetic energy injection, using winds instead of ejecta. This new scheme can change the interpretation of our results has it can modify the amount of gas outflowing from halos and change the way radiation escapes.

6 Acknowledgment

This work is supported by the ANR ORAGE grant ANR-14-CE33-0016 of the French Agence Nationale de la Recherche.

References

Aubert, D., Deparis, N., & Ocvirk, P. 2015, Monthly Notices of the Royal Astronomical Society, 454, 1012
Dalla Vecchia, C. & Schaye, J. 2012, Monthly Notices of the Royal Astronomical Society, 426, 140
Dubois, Y. & Teyssier, R. 2008, in Supernova Feedback in Galaxy Formation, Vol. 390, 388
Kay, S. T., Pearce, F. R., Frenk, C. S., & Jenkins, A. 2002, Monthly Notices of the Royal Astronomical Society, 330, 113
Kennicutt, J. 1998, The Astrophysical Journal, 498, 541, arXiv: astro-ph/9712213
Leitherer, C., Schaerer, D., Goldader, J. D., et al. 1999, The Astrophysical Journal Supplement Series, 123, 3
Planck Collaboration, Ade, P. A. R., Aghanim, N., et al. 2015, ArXiv e-prints, 1502, arXiv:1502.01589
Rasera, Y. & Teyssier, R. 2006, Astronomy and Astrophysics, 445, 1
Springel, V. & Hernquist, L. 2003, Monthly Notices of the Royal Astronomical Society, 339, 289
Stinson, G., Seth, A., Katz, N., et al. 2006, Monthly Notices of the Royal Astronomical Society, 373, 1074